Efficient organic solar cells based on a double *p-i-n* architecture using doped wide-gap transport layers

J. Drechsel,[a] B. Männig, F. Kozlowski, M. Pfeiffer, and K. Leo
Institut für Angewandte Photophysik, Technische Universität Dresden, D-01062 Dresden, Germany

H. Hoppe
Linz Institute for Organic Solar Cells (LIOS), Physical Chemistry, Johannes Kepler University, A-4040 Linz, Austria

(Received 4 January 2005; accepted 13 April 2005; published online 7 June 2005)

The use of doped wide-gap charge transport layers with high conductivity and low absorption in the visible range enables one to achieve high internal quantum efficiencies and to optimize the devices with respect to optical interference effects. Here, it is shown that this architecture is particularly useful for stacking several cells on top of each other. The doping eases the recombination of the majority carriers at the interface between the cells, whereas the recombination centers are hidden for excitons and minority carriers. By stacking two *p-i-n* cells both with a phthalocyanine-fullerene blend as photoactive layer, a power efficiency of up to 3.8% at simulated AM1.5 illumination as compared to 2.1% for the respective single *p-i-n* cell has been achieved. Numerical simulations of the optical field distribution based on the transfer-matrix formalism are applied for optimization. The concept paves the way to even higher efficiencies by stacking several *p-i-n* cells with different photoactive materials that together cover the full visible spectrum. © *2005 American Institute of Physics*. [DOI: 10.1063/1.1935771]

Several approaches to all-organic solar cells have been reported in the last few years.[1–5] All of them make use of the transformation of photogenerated excitons into free charge carriers at donor-acceptor heterojunctions. If devices are based on a heterojunction between two layers of neat materials,[1,2,5,6] excitons have to diffuse toward the interface to get separated. Here, only excitons being created within the exciton diffusion length can contribute to the photocurrent. This approach is mainly limited by the typically small exciton diffusion length in organic materials. To overcome this limitation, bulk heterojunctions were developed for various systems (polymers and small molecules).[4,7–10] Unfortunately, this concept has also its drawback. Bulk generated charge carriers need to percolate within the bulk blend toward their specific electrodes. That may lead to reduced charge carrier mobility by the intermixing of two compounds[11] which again limits the range of active layer thickness accessible without significant recombination losses.

An approach to circumvent this trade-off between losses by limited absorption for thin layers and recombination losses for thicker layers was introduced by Hiramoto *et al.*[2] who demonstrated the stacking of single heterojunction cells on top of each other. Yakimov *et al.*[12] improved this concept by stacking up to five single heterojunction cells on top of each other reaching a maximum power efficiency of 2.5% already for the double stacked cell. Similarly, we have shown the stacking of two *p-i-n* type bulk heterojunction solar cells on top of each other.[13,14] As stacked cells without separate contacts for the individual cells represent a series connection of two diodes, the open-circuit voltages (V_{OC}) simply add up. However, the short-circuit photocurrent of the stacked cell is basically limited by the lowest of the two individual cells. Balancing the contributions is further complicated by optical interference effects that can lead to different optical field strengths in the photoactive regions of the individual cells.

The basis of our stacked solar cells are single *p-i-n* cells based on a bulk heterojunction made of ZnPc:C_{60} blends as photoactive layers.[13–15] Those show rather encouraging power efficiencies of about 2% and already profit from the ability to shift the photoactive layer into the maximum of the optical interference pattern by adjusting the thickness of the transparent highly conductive transport layers. Simulated absorption profiles obtained by the one-dimensional (1D) transfer-matrix formalism (TMF) (Refs. 16 and 17) show reasonable agreement with experimental results.[14,15] It turns out that it is even more relevant for stacked cells to adjust the positions of all photoactive layers with respect to the maxima of the optical field distribution. To find the optimum combination of layer thicknesses, we again make use of numerical simulations of the optical field distribution based on the TMF.

As a key feature of the cells, organic doping of wide-gap transport materials based on the coevaporation of two organic compounds[18–20] is applied (typical dopant content: 1–4 mol %). The hole transporting materials N, N′-diphenyl-N,N′-bis(3-methylphenyl)-[1,1′-biphenyl]-4, 4′-diamine (MeO-TPD) is doped by the strong electron acceptor tetrafluorotetracyano-quinodimethane.[18,19] *n*-type doping of the electron transporting matrices C_{60} is based on cationic dyes, such as rhodamine B or their leuko base (leuko crystal violet) as a precursor.[20] The devices have been prepared on commercial semitransparent indium tin oxide (ITO)-coated glass substrates with a surface resistance of $\leqslant 50\ \Omega$/square. For stability reasons, in some of the samples, a PEDOT:PSS layer was spin cast onto the ITO before further processing in a vacuum. Current-voltage (I-*V*) characteristics have been taken *in situ* or in an inert nitrogen atmosphere.

[a]Electronic mail: drechsel@iapp.de

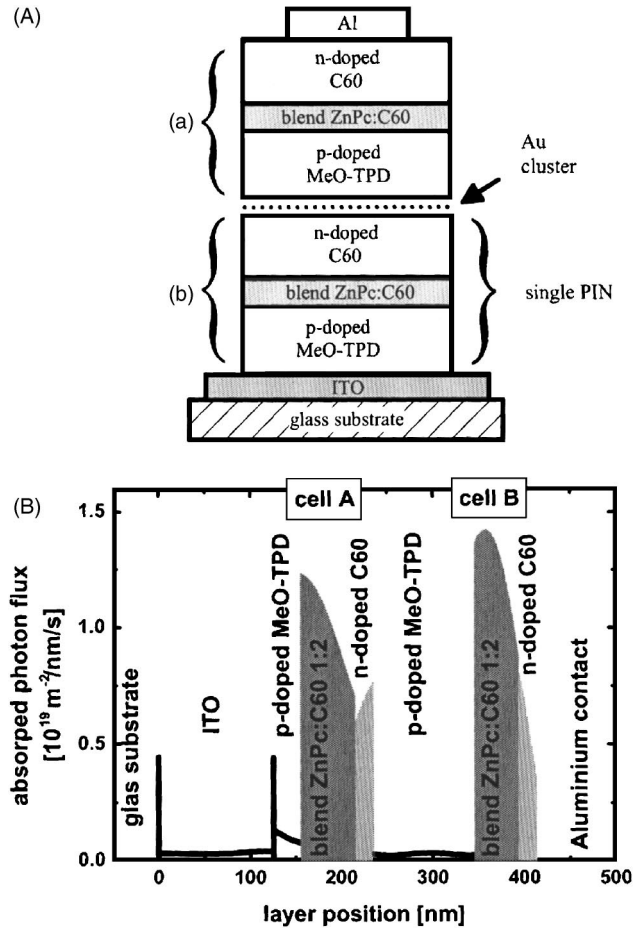

FIG. 1. Basic concept of a *p-i-n*-type organic solar cell with an active layer sandwiched between *p*- and *n*-type wide-gap transport layers: (a) The general layer sequence and (b) calculated absorbed photon flux profile at an illumination of 130 mW/cm^2 AM1.5 based on a nominal optimized device structure. It includes the contribution from adjacent C_{60} layers to the photocurrent. Under the assumption of 100% internal quantum efficiency, the integrated absorbed photon flux within the photoactive blend layers results in a maximum photocurrent of 9.8 mA/cm^2. If the contributions from the adjacent C_{60} layers are additionally taken into account, a maximum of 12.0 mA/cm^2 can be reached.

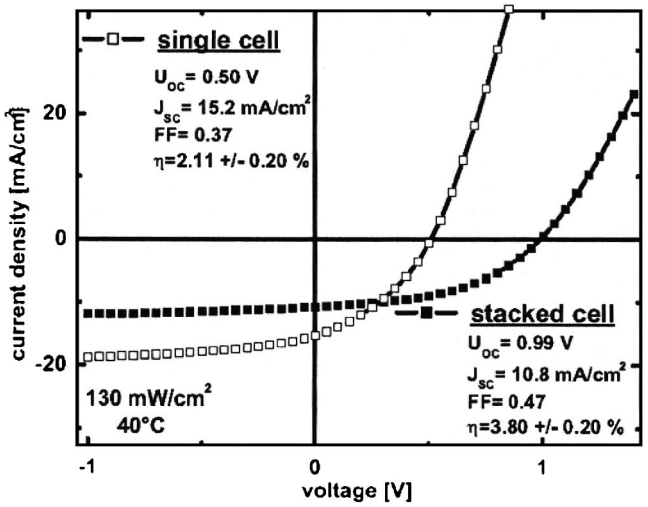

FIG. 2. *I-V* characteristics of single and tandem *p-i-n* solar cells under 130 mW/cm^2 simulated AM 1.5 solar illumination. The tandem cell has an optimized device structure according to the simulation shown in Fig. 1, and the single cell is identical to the bottom cell in the tandem configuration (Cell A) prepared simultaneously. The performance parameters are given.

Figure 1(a) depicts the device structure for a double stacked *p-i-n* cell. Those tandem cells are comprised of two single *p-i-n* cells with an ultrathin metal layer[14] in between that grow in a discontinuous way forming metal clusters.[2,12] Those induce favorable gap states and interface dipoles, and ease recombination and generation at the interface at reverse and forward bias voltage, respectively. For the charge transport materials MeO-TPD and C_{60} used here, the introduction of the metal clusters *and* doping of both adjacent layers is essential to get reasonable tandem cells.[14] However, the cluster morphology of the metal interlayer is not essential for this concept. In fact, we found that—in spite of the nominally high electron injection barrier to C_{60}—even solid gold layers form quasi-ohmic tunneling contacts to both *p*-doped MeO-TPD and *n*-doped C_{60}.

In the following, we describe the basic assumptions of the optical simulations and the strategy to find the optimum tandem cell configuration. Optical constants of all layers have been determined independently.[14] Due to the low dopant concentrations, we neglect a possible influence of the doping ratio on the optical constants. For simplicity, the interfacial gold layer has been assumed to be solid. We assume that exciton generation in the neat C_{60} layers contributes to the photocurrent[15] as these excitons can diffuse to the blend layer to get separated into free charge carriers by hole transfer to ZnPc.

To reduce the number of free parameters, several thicknesses are fixed *a priori*. As is known from former experiments,[14] the thickness of the ITO and the adjacent hole transport layer have a minor influence on the optical field distributions. They are fixed to 125 nm for the ITO and 30 nm for the MeO-TPD. The maximum thickness of the photoactive ZnPc:C_{60} layers (blend ratio of 1:2) is set to 60 nm. As was determined in a series of independent experiments, thicker blend layers show reduced fill factors and high recombination losses. Furthermore, we keep the thickness of the *n*-doped C_{60} layers as thin as possible to minimize parasitic absorption losses. To make sure that they are still considerably thicker than the depletion layer that may be formed at its interface, we chose 20 nm C_{60} without further optimization. For the cell directly below the reflective aluminum top contact (Cell B), the 20 nm doped C_{60} layer already represents a spacer close the optimum in respect to the optical interference maximum. Thus, only two free parameters are left, namely the thickness of the blend layer of Cell B and the thickness of its hole transport layer which determines the spacing between the photoactive layers of the two cells.

The aim of the optimization is to find a configuration where both individual *p-i-n* cells are able to generate similar photocurrent. Its value should be as high as possible. As a result, the absorbed photon flux at an illumination intensity of 130 mW/cm^2 AM1.5 is given in Fig. 1(b) for a nominal optimized structure within the given limits. In detail, the layer sequence is ITO/30 nm *p*-doped MeO-TPD/60 nm ZnPc:C_{60} blend (molar ratio of 1:2)/20 nm *n*-dopedC_{60}/0.5 nm Au/125 nm *p*-doped MeO-TPD/50 nm ZnPc:C_{60} blend (molar ratio of 1:2)/20 nm *n*-doped C_{60}/100 nm Al. Obviously, the absorption takes place mainly in the ZnPc:C_{60} blend layers and in the electron transport layers consisting of C_{60}. Assuming 100% internal quantum efficiency, the integration of current generation of the blend layers leads to a photocurrent density of

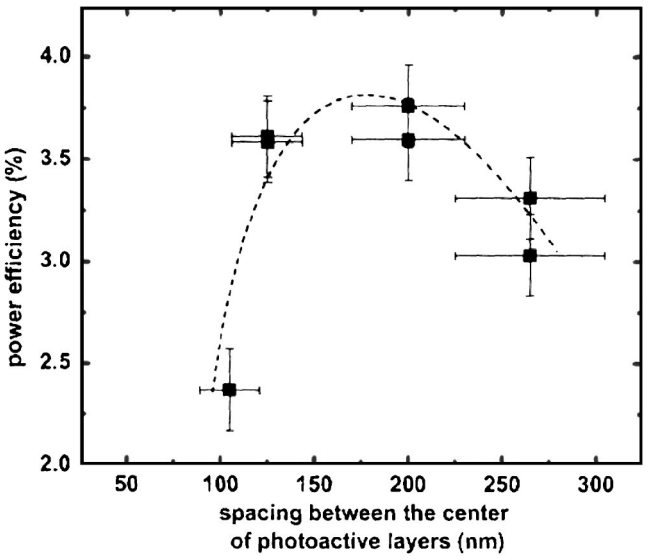

FIG. 3. Power efficiencies for *p-i-n* tandem cells plotted vs the distance between the centers of the photoactive layers. The device structure has been kept constant except for the separating hole transport layer between Cells A and B. The dashed line represents a guide for the eyes.

9.8 mA/cm^2 in Cell A and 9.8 mA/cm^2 in Cell B, respectively.

With the full contribution of the adjacent C_{60} layers, the photocurrent is approximately 12.0 mA/cm^2 for both *p-i-n* cells. The *I-V* characteristics of the nominal optimized tandem cell are given in Fig. 2, together with characteristics of the first single cell (Cell A). The tandem cell exhibits a significantly higher power efficiency of $3.8\pm0.2\%$ compared to the single *p-i-n* cell ($2.1\pm0.2\%$) under 130 mW/cm^2 simulated AM 1.5 illumination. The open-circuit voltage of $V_{OC}=0.99$ V is doubled as compared to the single *p-i-n* cell ($V_{OC}=0.50$ V). The short-circuit current of the tandem is reduced, but still clearly exceeds one-half of the value of the single cell. We also note a remarkably improved fill factor of 0.47 for the tandem cell, as compared to 0.36 for the single cell which we attribute mainly to the reduced impact of the series resistance. Additionally, the smaller thickness of the active blend layer (50 nm) in Cell B lowers the overall recombination losses of the complete device.

The *I-V* characteristic of the tandem cell shows a reasonable saturation of the photocurrent with negative voltage. As both geminate and nongeminate recombination losses should be field dependent, we suggest that this saturation current corresponds to a recombination-free situation, i.e., close to 100% internal quantum efficiency. If we compare the saturation value of 12.5 mA/cm^2 at 130 mW/cm^2 illumination with the simulated maximum photocurrents of 9.8 mA/cm^2 (exclusively blend layer) and 12.0 mA/cm^2 (blend layer and adjacent C_{60}), we conclude that indeed the neat C_{60} contribute to the photocurrent. The reasonable agreement between experiment and calculation confirms the model.

In Fig. 3, the power efficiencies of a series of stacked *p-i-n* cells are depicted as a function of the distance of the centers of the photoactive blend layers of the two cells. Except for the thickness of the hole transport layer of Cell B (doped MeO-TPD), all thicknesses of transport layers and photoactive layers have been kept constant. A maximum shows up around the proposed optimized configuration that confirms the application of the optimization procedure.

In conclusion, we have demonstrated high efficiency organic photovoltaic devices by stacking *p-i-n* type cells. To create a low loss contact between the stacked cells, both the doping of the wide-gap transport layers and the introduction of gold clusters as recombination and generation centers are essential. A major advantage of the concept is that the photoactive layers can be placed in an optimum position with respect to the optical interference pattern by adjusting the thickness of the doped wide-gap transport layers. The tandem cell reaches $3.8\pm0.2\%$ power conversion efficiency which is a significant improvement compared to single *p-i-n* cells. A further improvement is expected already by using more conductive ITO as the cells show indications of a series resistance that does not arise from the organic transport layers (cf. Ref. 21). Engineering the morphology and transport properties in the photoactive blend layers will be addressed in future work. Application to commercially interesting efficiencies is anticipated if we stack two or more cells with complementary absorption to cover the complete visible and near-infrared range of the solar spectrum.

The authors thank the German Secretary for Education and Research (BMBF, FKZ 01SF0027) for financial support.

[1] C. W. Tang, Appl. Phys. Lett. **48**, 183 (1986).
[2] M. Hiramoto, M. Suezaki, and M. Yokoyama, Chem. Lett. **1990**, 327, 1990.
[3] D. Wöhrle and D. Meissner, Adv. Mater. (Weinheim, Ger.) **3**, 129 (1991).
[4] S. E. Shaheen, C. J. Brabec, N. S. Sariciftci, F. Padinger, T. Fromherz, and J. C. Hummelen, Appl. Phys. Lett. **78**, 841 (2001).
[5] P. Peumans, A. Yakimov, and S. R. Forrest, J. Appl. Phys. **93**, 3693 (2003).
[6] T. Stübinger and W. Brütting, J. Appl. Phys. **90**, 3632 (2001).
[7] M. Hiramoto, H. Fujiwara, and M. Yokoyama, Appl. Phys. Lett. **58**, 1062 (1991).
[8] M. Hiramoto, H. Fujiwara, and M. Yokoyama, J. Appl. Phys. **72**, 3781 (1992).
[9] J. Rostalski and D. Meissner, Sol. Energy Mater. Sol. Cells **61**, 87 (2000).
[10] V. Dyakonov, J. Parisi, and N. S. Sariciftci, *Organic Photovoltaics: Concepts and Realization*, edited by C. J. Brabec (Springer, Berlin, 2003).
[11] E. J. Meijer, D. M. De Leeuw, S. Setayesh, E. van Veenendaal, B.-H. Huisman, P. W. M. Blom, J. C. Hummelen, U. Scherf, and T. M. Klapwijk, Nat. Mater. **2**, 678 (2003).
[12] A. Yakimov and S. R. Forrest, Appl. Phys. Lett. **80**, 1667 (2002).
[13] J. Drechsel, B. Männig, F. Kozlowski, D. Gebeyehu, A. Werner, M. Koch, K. Leo, and M. Pfeiffer, Thin Solid Films **451**, 515 (2004).
[14] B. Männig, J. Drechsel, D. Gebeyehu, P. Simon, F. Kozlowski, A. Werner, F. Li, S. Grundmann, S. Sonntag, M. Koch, K. Leo, M Pfeiffer, H. Hoppe, D. Meissner, N. S. Sariciftci, I. Reidel, V. Dyakonov, and J. Parisi, Appl. Phys. A: Mater. Sci. Process. **79**, 1 (2004).
[15] J. Drechsel, B. Männig, D. Gebeyehu, M. Pfeiffer, K. Leo, and H. Hoppe, Org. Electron. **5**, 175 (2004).
[16] L. A. A. Pettersson, L. S. Roman, and O. Inganas, J. Appl. Phys. **86**, 487 (1999).
[17] H. Hoppe, N. Arnold, D. Meissner, and N. S. Sariciftci, Thin Solid Films **451**, 589 (2004).
[18] M. Pfeiffer, A. Beyer, B. Plönnigs, A. Nollau, T. Fritz, K. Leo, D. Schlettwein, S. Hiller, and D. Wöhrle, Sol. Energy Mater. Sol. Cells **63**, 83 (2000).
[19] B. Männig, M. Pfeiffer, A. Nollau, X. Zhou, P. Simon, and K. Leo, Phys. Rev. B **64**, 195208 (2001).
[20] A. G. Werner, F. Li, K. Harada, M. Pfeiffer, T. Fritz, and K. Leo, Appl. Phys. Lett. **82**, 4495 (2003).
[21] S. Udicha, J. Xue, B. P. Rand, and S. R. Forrest, Appl. Phys. Lett. **84**, 4218 (2004).